ELSEVIER

Catalysis Today 54 (1999) 181–190

CATALYSIS TODAY

www.elsevier.com/locate/cattod

Catalytic combustion of methane over copper- and manganese-substituted barium hexaaluminates

P. Artizzu-Duart [a,1], Y. Brullé [b], F. Gaillard [a], E. Garbowski [a], N. Guilhaume [a,*], M. Primet [a]

[a] *Laboratoire d'Application de la Chimie à l'Environnement, UMR 5634, Université Claude Bernard Lyon 1, Bât. 303, 43 Boulevard du 11 Novembre 1918, F-69622 Villeurbanne Cedex, France*

[b] *Gaz de France, Direction de la Recherche, CERSTA, 361 Avenue du Président Wilson, BP 33, F-93211 Saint-Denis La Plaine Cedex, France*

Abstract

Copper- and manganese-substituted barium hexaaluminates were prepared by sol–gel method from metal alkoxides. The preparation conditions strongly influence the textural properties of the solids obtained. Manganese and copper occupy different crystallographic sites in the hexaaluminate structure: Mn^{3+} ions are located in octahedral sites, while Cu^{2+} enters only tetrahedral positions. The Cu sites are intrinsically more active than Mn sites for methane combustion, but the Cu-based catalysts are penalized by lower surface areas and by the lower limit of copper incorporation in the hexaaluminate matrix: manganese substitution for aluminium is possible up to ≈3 Mn per unit cell, while copper substitution is limited to about 1.3 Cu per unit cell. The catalytic activity of the Mn-substituted barium hexaaluminates increases with Mn substitution, the optimum composition being obtained when about 3 Mn ions per unit cell are incorporated, as regards the activity and the resistance to ageing at 1200°C in the presence of steam. This is related not only to the Mn content, but also to the higher Mn^{3+}/Mn^{2+} ratio when the amount of manganese introduced increases, as shown by TPR and Auger parameter measurements. The catalytic activity can be correlated with the fraction of reducible manganese species.

Keywords: Methane combustion; Barium hexaaluminate; Manganese; Copper; Thermal stability; High temperature combustion

1. Introduction

The catalytic combustion of hydrocarbons is a promising technology for energy production, since it produces very low amounts of CO and unburned hydrocarbons, while the thermal formation of NO_x is practically suppressed, because the operating temperatures are lower than in a flame. Methane combustion is of particular interest because it is the main component of natural gas, for which large world reserves are available, and which generally contains low amounts of sulfur- and nitrogen-containing compounds. For the high temperature stage of gas turbines, a high thermal stability of the catalysts is required, because temperatures in the 1000–1400°C range are reached. Barium hexaaluminate, $BaAl_{12}O_{19}$, is at present one of the most stable solids in terms of surface area maintained after high temperature treatments [1]. It may be doped with active cations of transition metals (Cr, Mn, Fe, Co, Ni), leading to highly resistant combustion catalysts [2]. The present study compares the properties of copper- and manganese-substituted barium hexaaluminates as catalysts for methane combustion, in relation with their physicochemical properties.

* Corresponding author. Fax: +33-478-94-19-95

E-mail address: guilhaum@univ-lyon1.fr (N. Guilhaume)

[1] Present address: Battelle, Geneva research centres, 7 Route de Drize, CH-1227 Carouge-Geneva, Switzerland.

0920-5861/99/$ – see front matter
PII: S0920-5861(99)00179-0

Table 1
Chemical composition of catalysts and crystalline phases identified by XRD

Code name	Catalyst composition from chemical analyses	Phases detected in the XRD patterns[a]
Mn catalysts		
BaMn	$BaMn_{0.97}Al_{11}O_x$	Ba–β-Al_2O_3, α-Al_2O_3 (traces)
BaMn2	$BaMn_{1.9}Al_{10}O_x$	Ba–β-Al_2O_3, $BaAl_2O_4$(traces), α-Al_2O_3 (traces)
BaMn3	$BaMn_{2.7}Al_{10}O_x$	Ba–β-Al_2O_3
BaMn4	$BaMn_4Al_8O_x$	Ba–β-Al_2O_3, Mn_2O_3, $BaAl_2O_4$ (traces)
Cu catalysts		
BaCu	$BaCuAl_{13.3}O_x$	Ba–β-Al_2O_3, α-Al_2O_3 (traces)
BaCu2	$BaCu_{2.1}Al_{11.9}O_x$	Ba–β-Al_2O_3, $CuAl_2O_4$

[a]Ba–β-Al_2O_3: $BaAl_{13.2}O_{20.8}$: JCPDS-ICDD file No. 33-128.

2. Experimental

2.1. Preparation of catalysts

The substituted barium hexaaluminates $BaM_xAl_{12-x}O_{19-\delta}$ (M = Cu, x = 1–2; M = Mn, x = 1–4) were prepared by a sol–gel method as suggested by Machida et al. [2]. The preparations were performed under dry argon using standard Schlenk techniques. Isopropanol was dried and distilled before use. Metallic barium (1.7 g) and aluminium isopropoxide (31.8 g) were suspended in 400 ml of isopropanol. The suspension was refluxed for 3 h, then cooled to room temperature. The metal alkoxides mixture was hydrolyzed with an under-stoichiometric amount of water ($xH_2O/M(OiPr)_x = 0.5$, in which $x = 2$ for M = Ba and $x = 3$ for M = Al), diluted in isopropanol and dripped slowly. For the Cu- and Mn-containing solids, the required amount of $Cu(NO_3)_2{\cdot}3H_2O$ or $Mn(NO_3)_2{\cdot}4H_2O$ was dissolved in a water/alcohol mixture and added during the hydrolysis step. A gel was formed rapidly, and allowed to process at ambient temperature for 15 h The solvents were evaporated under reduced pressure, the powders obtained were dried at 120°C, followed by calcination in a quartz cell at 1200°C for 24 h under a flow of oxygen. This temperature was necessary to ensure the complete formation of the hexaaluminate phase. The catalysts issued from this calcination will be referred to as *fresh catalysts*. The code name of each synthesized solid, as well as the exact compositions, determined by chemical analyses are presented in Table 1.

The ageing treatment was performed at 1200°C for another 24 h, under a flowing O_2/N_2 mixture (5 vol.% O_2) containing 6 vol.% water vapor. The combustion of hydrocarbons produces water vapor which is known for its strong sintering effect on metal oxides at high temperature [3]. This procedure represents a quick simulation for the ageing of a combustion catalyst under working conditions for long periods. The resulting solids are referred to as *aged catalysts*.

2.2. Physicochemical analysis

Chemical analysis was performed by Atomic Absorption Spectroscopy after dissolution of the solids in a mixture of concentrated acids ($HF + HCl + HNO_3$).

X-ray diffraction patterns were recorded with a SIEMENS D500 diffractometer using the nickel filtered Cu $K_{\alpha 1}$ line at 1.5406 Å. The spectra were recorded between 5 and 70° (2θ) with a scan rate of 1.2° min^{-1}. Silicon powder (60 mesh, 5 wt.%) was added to the samples as an internal standard. The phases were identified by comparison with the JCPDS-ICDD files. The cell parameters were calculated using a least-squares method, on the basis of the positions of 16–24 peaks.

Specific surface areas were measured by nitrogen adsorption at 77 K using the multipoint BET method. The solids were treated at 500°C under vacuum (10^{-5} Torr) for 2 h prior to nitrogen adsorption.

UV–VIS–NIR diffuse reflectance spectra were recorded with a Perkin–Elmer Lambda 9 spectrometer with an integrating sphere allowing scanning from 200 to 2500 nm. $BaSO_4$was used as reference.

Temperature programmed reduction (TPR) of the catalysts was performed under 1 vol.% H_2 in argon, with a temperature ramp of 8° C min^{-1}, starting from

room temperature up to 1000°C. Hydrogen consumption was monitored by an on-line TCD detector, and the percentage of copper reduction could be determined with an accuracy of 6–8%. The samples were pretreated in air at 400°C for 1 h, and cooled to ambient temperature under argon before measurements.

The surface composition of copper catalysts was studied by XPS with a VG-type ESCA III spectrometer, using Al K_α radiation (1486.6 eV). The binding energies were corrected with respect to the C 1*s* peak of carbon at 284.6 eV.

The XPS data on Mn-substituted samples were recorded on a RIBER SIA 200 multitechnique (XPS, AES, ISS) spectrometer, equipped with a MAC2 analyser. Non-monochromatised Al K_α radiation from a dual anode (Mg/Al) system was used as excitation source. The maximum of the C 1*s* peak envelope corresponding to carbon atoms bonded to other carbon and hydrogen atoms was assumed to be at 285.1 eV, as determined in a previous study of several Mn/Al_2O_3 catalysts [4].

The energies of Mn 2*p*3/2 and Mn 2*p*1/2 electrons are respectively similar for Mn oxides and $MnAl_2O_4$ and lay within a range 1–1.5 eV [4–5]. This, and the fact that referring to C 1*s* is not reliable over a range of ± 0.5 eV led us to use α', the modified Auger parameter [6], to determine the oxidation state of the incorporated Mn:

$$\alpha' = \mathrm{KE\,MnL_3M_{2,3}M_{4,5}} - \mathrm{KE\,Mn2}p3/2 + h\nu\ (\mathrm{Al}\ K_\alpha)$$

where KE is the kinetic energy of the considered electron.

The catalytic activity in methane combustion was measured on 0.50 g of samples placed in a quartz microreactor. The solids were first pretreated in O_2 at 400°C during 1 h, cooled to 350°C, then the reactant gas mixture consisting of 1 vol.% CH_4, 4 vol.% O_2 and 95 vol.% N_2 was admitted. The total flow ($6.4\,l\,h^{-1}$) corresponds to a gas space velocity of 20,000–25,000 h^{-1}. The temperature was increased by steps of 50°C between 350 and 800°C, and the conversion was measured isothermally at each temperature during 3 h, in order to check any time-on-stream deactivation. CH_4, CO_2 and eventually CO were separated on a Carbosieve S chromatographic column, and analyzed as described in Ref. [7].

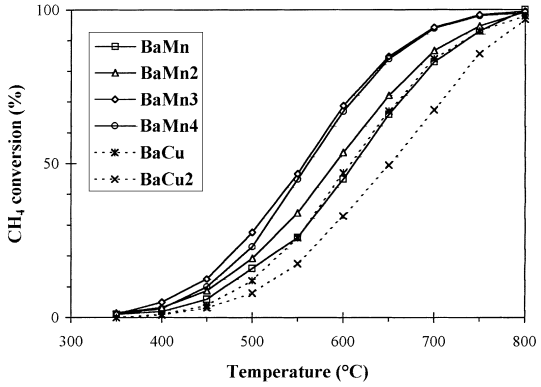

Fig. 1. Methane conversion versus temperature over the Cu- and Mn-substituted barium hexaaluminates (fresh catalysts). Conditions: 1% CH_4, 4% O_2, balance N_2, total flow rate $6.4\,l\,h^{-1}$, 0.50 g catalysts.

3. Results and discussion

3.1. Activity for methane oxidation

The methane conversions on Mn- and Cu-substituted barium hexaaluminates are shown in Fig. 1. The code name and the corresponding compositions of the catalysts are indicated in Table 1. All catalysts are active in the temperature range of 350–800°C, and the only product detected is CO_2. The monosubstituted catalysts, BaMn and BaCu, have very similar conversions. With 2 and 3 Mn ions introduced, the conversion temperatures are shifted to lower values, but the introduction of the fourth Mn does not improve the activity. Since the surface areas of the solids are different, the intrinsic rates of reaction (μmol CH_4 transformed per

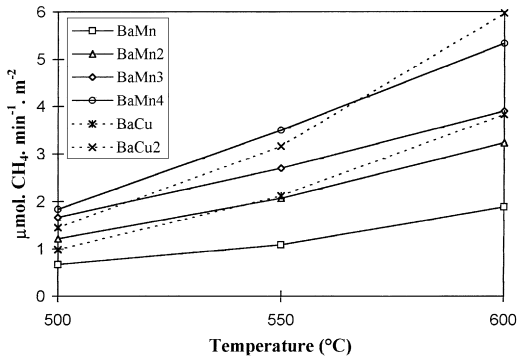

Fig. 2. Reaction rates (μmol CH_4 transformed per minute and per square meter of catalyst) at 500, 550 and 600°C, on fresh catalysts.

minute and per square meter of catalyst) in the low conversion domain are reported in Fig. 2. The activity of the Mn-based catalysts increases regularly with the Mn loading, although not exactly proportionally to the Mn amount. The BaMn4 catalyst is more active (intrinsically) than BaMn3, but the conversion of methane on BaMn4 is slightly lower than on BaMn3 (Fig. 1) because its surface area is lower. The copper catalysts, at the same atomic substitution ratio, are more active than the Mn-based catalysts, but they are penalized by their lower surface areas.

3.2. Characterization of the fresh catalysts

The sol–gel synthesis of the substituted barium hexaaluminates leads to the formation of barium–β-alumina as the main phase for all catalysts (Table 1). Traces of α-alumina are detected in some cases, in agreement with the slight excess of Al isopropoxide introduced during the synthesis and the excess Al found in the corresponding chemical analyses.

The XRD pattern of the unsubstituted barium hexaaluminate corresponds well to that of a phase of composition $BaAl_{13.2}O_{20.8}$ (ICDD file 33-128). It is well established that barium hexaaluminate $BaAl_{12}O_{19}$ is not a single phase, but consists in a mixture of two phases, called β_I and β_{II}, with compositions $BaAl_{14}$ (Ba-poor) and $BaAl_9$ (Ba-rich), respectively [8]. Powder diffraction patterns of these two phases are very similar, only the relative intensities of some diffraction lines are slightly different. The calculated '*a*' cell parameter of our sample is in agreement with a nearly equimolar mixture of β_I and β_{II} phases ($a = 5.5936$ Å [8]).

Incorporation of Mn and Cu transition metal cations, which are larger than Al^{3+} ions [9], is expected to result in an increase of the '*a*' cell parameter: this is indeed observed in Table 2. For the manganese-based catalysts, no Mn-containing phase is detected in the XRD patterns up to 3 Mn per unit cell. When the substitution reaches 4 Mn per unit cell, the main diffraction lines of Mn_2O_3 appear. The '*a*' cell parameter increases regularly up to 4 Mn, however, suggesting that a little more than 3 Mn ions can be incorporated. The variation is not linear (Fig. 3), and this can be due to the fact, as will be seen later,

Table 2
Specific surface areas of catalysts after calcination at 1200°C, and '*a*' cell parameters calculated from XRD patterns.

Catalyst	Surface area ($m^2\ g^{-1}$)	'*a*' Cell parameter (Å)
$BaAl_{12.3}O_x$	11	5.591
Mn catalysts		
$BaMn_{0.97}Al_{11}O_x$	20	5.625
$BaMn_{1.9}Al_{10}O_x$	14	5.647
$BaMn_{2.7}Al_{10}O_x$	14	5.661
$BaMn_4Al_8O_x$	10	5.674
Cu catalysts		
$BaCuAl_{13.4}O_x$	11	5.614
$BaCu_{2.1}Al_{11.9}O_x$	5	5.620

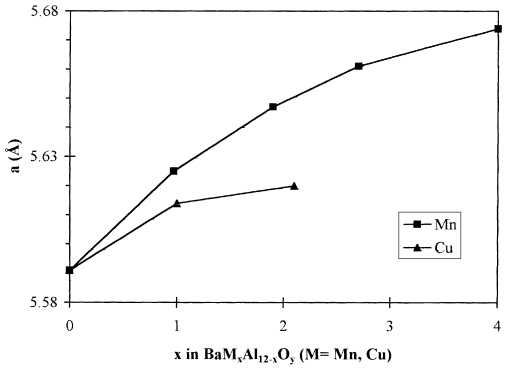

Fig. 3. Variation of '*a*' unit cell parameter with transition metal substitution.

that the manganese ions are present as a mixture of Mn^{2+} and Mn^{3+} (Mn^{3+} being slightly smaller), with a Mn^{3+}/Mn^{2+} ratio increasing with the amount of manganese introduced. The limit of Mn incorporation appears to be between 3 and 4 Mn ions per unit cell. Traces of $BaAl_2O_4$ are also observed in the patterns of the BaMn2 and BaMn4 catalysts, indicating that the formation of the hexaaluminate phase was not complete. TEM examination with EDX analyses were performed on the monosubstituted solid: although the particles are similar in shape, two compositions are detected in which the Ba/Mn/Al ratios are 1/0.78/11.6 and 1/0.8/6, respectively. The Ba/Mn ratio is close to that expected from chemical analysis (0.97), but the Ba/Al ratio is not constant, and could correspond to the β_I and β_{II} phases.

In the case of copper catalysts, the limit for copper incorporation seems to be between 1 and 2 Cu^{2+} ions

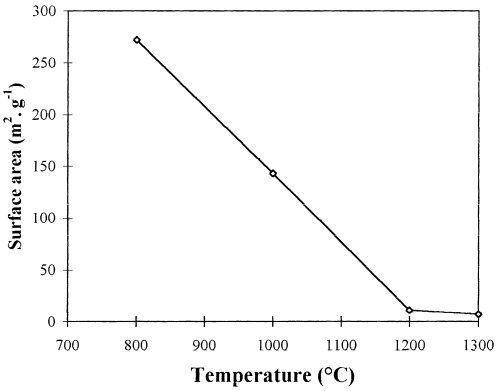

Fig. 4. Surface area of the xerogel precursor of $BaAl_{12}O_{19}$ following calcination at 800 and 1000°C for 5 h, and at 1200°C for 24 h.

per unit cell. By linear extrapolation of the first part of the curve in Fig. 3, the expansion of the cell parameter suggests that a maximum of 1.3 Cu^{2+} per unit cell can be incorporated in the hexaaluminate matrix. The excess copper forms copper aluminate $CuAl_2O_4$ (Table 1). This was also confirmed by TEM/EDX analysis: for the monosubstituted sample all analyzed particles have the mean composition Ba/Cu/Al = 1/1/11, while in the case of the bisubstituted two types of particles are detected, corresponding to the $BaCu_{1.04}Al_{10.4}$ and $CuAl_{2.4}$ formulas, respectively.

The specific surface areas remain relatively high after calcination at 1200°C for 24 h (Table 2), in the 10–20 $m^2\,g^{-1}$ range. The starting powders obtained by this sol–gel method have very high surface areas: for the barium hexaaluminate phase, the powder was $\approx$270 $m^2\,g^{-1}$ after calcination at 800°C, temperature at which the solid was still completely amorphous. The evolution of the surface area after various calcination temperatures between 800 and 1300°C is presented in Fig. 4. After calcination at 1000°C, the powder is still amorphous, and the surface area has been reduced by a factor of $\approx$2. Crystallization is obtained at 1200°C, and is accompanied with a strong decrease in the surface area which is now 11 $m^2\,g^{-1}$.

The surface area of the crystallized $BaAl_{12}O_{19}$ phase is related to the nature of the metal alkoxides used as precursors and to the properties of the gel formed upon hydrolysis: when Al- and Ba-isopropoxides are used, the reacting mixture *remains a suspension*, because aluminium isopropoxide is only moderately soluble in the parent alcohol, while barium isopropoxide is not [10]. A double metal alkoxide $BaAl_2(O^iPr)_8$ can be formed by reaction between the two metal alkoxides [10], which is much more soluble than the simple Ba and Al isopropylates, but the Ba/Al ratio of 1/12 used for the synthesis is not appropriate. The gel formed by hydrolysis is thus not homogeneous, and the precursor powder obtained after drying must be composed of particles which are heterogeneous in size and in composition. Since sol–gel methods are supposed to allow the preparation of homogeneous solutions of the precursors, and since the preparation is not described with much details in the Arai et al. papers (in particular the concentrations used for the synthesis), we investigated a different preparation method for the $BaAl_{12}O_{19}$ matrix: commercial aluminium sec-butylate ($Al(OC_4H_9)_3$) was reacted with barium 2-methoxyethoxide ($Ba(OCH_2CH_2OCH_3)_2$), which was prepared by reaction between barium metal and 2-methoxyethanol. The mixture of these two very soluble precursors is a clear solution, which leads to an homogeneous gel upon hydrolysis of the metal–alkoxide bonds. After evaporation of the solvent and calcination at 1200°C, the surface area of the Ba–β-Al_2O_3 phase obtained by this method is only 1 $m^2\,g^{-1}$.

The homogeneity of the precursors mixture seems an important factor for the resistance to sintering: actually, the solid resists better to high temperature sintering when the starting mixture is *not homogeneous*, while a very homogeneous xerogel sinters more easily. This is normal since powders with small particle sizes in a narrow distribution are more easy to sinter than heterogeneous powders [11]. The porous system formed during the gelation process in the two sol–gel syntheses is also probably different, because of the different metal alkoxides and solvents used, and may be a very important factor for the remaining surface area after formation of the hexaaluminate phase: in comparative syntheses of lanthanum hexaaluminates by various methods (sol–gel and coprecipitation), Ersson et al. [12] showed that the formation of large pores allowed the La-hexaaluminate to retain a larger surface area than when small pores were formed in the precursor powder.

Manganese incorporation in the hexaaluminate matrix (up to 3 Mn) allows a better resistance to

sintering, the surface areas of the $BaMn_x$ catalysts ($x = 1$–3) being somewhat higher than that of the $BaAl_{12}O_{19}$ phase alone (Table 2). Machida et al. [2] obtained a different result with Mn-substituted barium hexaaluminates: the surface area was maintained for 1 and 2 Mn ions, but decreased sharply when a third Mn ion was introduced, leading to a less active catalyst. The difference may arise from the concentrations of the precursors used in the preparation.

On the opposite, introduction of one copper ion does not modify the surface area, while the powder obtained upon introduction of a second copper ion has a lower surface area, probably because of the $CuAl_2O_4$ formation.

UV–VIS spectroscopy was used to investigate the coordination of the transition metals introduced in the hexaaluminate structure. The spectra of all Mn catalysts present an intense absorption band centered around 480 nm, which can be attributed to Mn^{3+} ions in octahedral position. No Mn^{3+} in tetrahedral position is detected in the 900–1000 nm region, nor Mn^{4+} ions which should present a band around 600 nm. Mn^{2+} ions, however, cannot be detected by this technique since their electronic transitions are too weak to be seen in the presence of Mn^{3+} ions. The intensity of the 480 nm band increases with Mn substitution, although not exactly linearly. The monosubstituted copper catalyst shows a broad band around 1600 nm, characteristic of copper ions in tetrahedral coordination. No transitions in the 600–900 nm range, corresponding to octahedral copper, are observed. The bisubstituted catalyst presents, in addition to the 1600 nm band of tetrahedral copper, a second band centered below 500 nm, which is present in the spectra of pure $CuAl_2O_4$ [13].

These results show that the Cu^{2+} and Mn^{3+} cations introduced in the hexaaluminate structure occupy different crystallographic sites: Mn^{3+} ions are found preferentially in octahedral positions, while Cu^{2+} ions occupy only tetrahedral sites. Mn^{2+} ions, however, may be also present but are not detected by this technique. This is in agreement with the results of Groppi et al. [14], who studied the incorporation of manganese in barium hexaaluminate (Mn/Ba ratio varying from 0.5 to 3) by XANES spectroscopy: they showed that at low Mn concentration, Mn preferentially enters the structure in tetrahedral Al(2) sites, with dominant oxidation state 2+. The same conclusion was deduced from X-ray analysis of a single crystal of Mn-substituted barium hexaaluminate (Mn/Ba ≈ 0.32) by Inoue et al. [15]: small amounts of Mn^{3+} and Mn^{2+} ions replace Al(2) in tetrahedral sites of the spinel block. The replacement of Al^{3+} by Mn^{2+} is allowed by a charge compensation mechanism associated with the reduction of Ba vacancies in the mirror plane of the structure [14]. On increasing the Mn content, the Ba sites are progressively saturated, and the charge compensation mechanism can no longer operate: Mn enters then the octahedral Al(1) sites and the dominant oxidation state is now 3+. This could be a reason for the limited copper substitution (about one Cu^{2+} per unit cell) in the hexaaluminate structure, since there is no possibility of increasing its oxidation state.

TPR under hydrogen was used to evaluate the reducibility of the manganese cations introduced in the barium hexaaluminate structure. The reducibility of the catalytic sites is an important property for metal oxide catalysts, since the oxidation of methane involves chemisorbed oxygen (Eley–Rideal mechanism), while lattice oxygen (Mars and Van Krevelen mechanism) dominates the oxidation process at higher temperatures [16]. The TPR experiments were performed starting from ambient temperature up to 1000°C, temperature at which the Mn^{3+} ions are supposed to be reduced into Mn^{2+}. Further reduction of Mn^{2+} into Mn^0 by hydrogen requires a temperature higher than 1200°C [4]. This means that only the manganese species involved in a Mn^{3+}/Mn^{2+} redox cycle are responsible for the catalytic activity in methane oxidation. The TPR profiles of the $BaMn_xAl_{12-x}O_{19-\delta}$ (M = Mn, $x = 1$–3) catalysts are shown in Fig. 5. The reduction is observed as a broad peak between 400 and 800°C. This temperature represents the end of the first reduction peak, and also corresponds to the temperature at which total conversion of methane is reached with all the Mn-based catalysts. When the temperature is further increased between 800 and 1000°C, a second reduction peak tends to appear, but this reduction is not finished at the end of the temperature ramp, so we only took into account the hydrogen consumption between 25 and ≈800°C, temperature at which the hydrogen consumption is minimum. The results are shown in Table 3. It appears that only a fraction of the manganese introduced in the hexaaluminate matrix is reducible under 800°C, and this fraction

Table 3
Hydrogen consumption at $T < 800°C$ in TPR experiments

Catalyst	H_2 consumed per gram catalyst (mmol)	Mn (total) per gram catalyst (mmol)	Mn^{3+} reduced[a] at $T < 800°C$ (%)
BaMn	0.104	1.220	17
BaMn2	0.363	2.130	34
BaMn3	0.679	3.103	44

[a]Based on a $Mn^{3+} + 1/2\ H_2 \rightarrow Mn^{2+} + H^+$ stoichiometry.

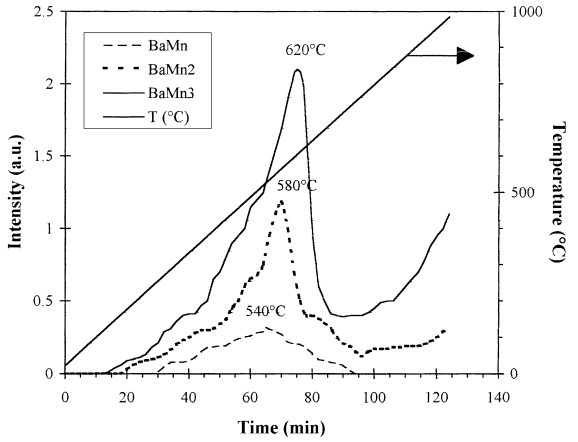

Fig. 5. H_2–TPR profiles of $BaMn_x$ catalysts ($x = 1$–3).

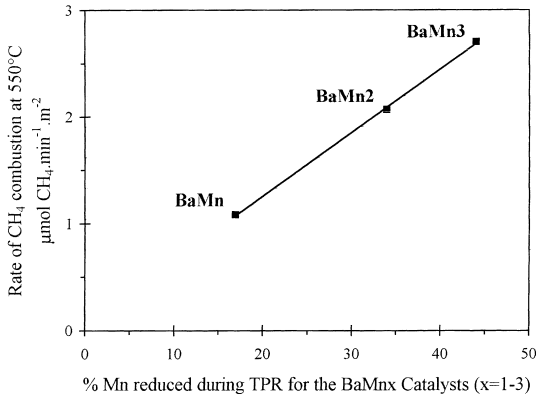

Fig. 6. Correlation between the catalytic activity and the amount of manganese reduced during the TPR experiments.

increases with the manganese amount introduced. This is consistent with the observation that Mn oxidation state tends to increase with Mn substitution [14–15]. In the case of the BaMn solid, the reduction is achieved before the end of the temperature ramp, so an average oxidation state of about 2.2 for manganese can be deduced from hydrogen consumption. For the other catalysts, the reduction is not completed at 985°C, and it is thus not possible to calculate an oxidation state for manganese, but the percentage of Mn reduced between ambient temperature and 800°C clearly increases. It is interesting to note that the temperatures required for Mn^{3+} reduction (maximum around 600°C) are high compared to the reduction of bulk oxides: Strohmeier and Hercules [4] report that bulk β-MnO_2, Mn_2O_3 and Mn_3O_4 are all reduced into MnO under hydrogen at temperatures lower than 250°C, MnO being stable under H_2 up to 1200°C. Maltha et al. [17], however, found higher reduction temperatures for bulk α-Mn_3O_4: 400–490°C according to the preparation method, in agreement with the results of Wang et al. (380–500°C) [18]. Finally, in the case of manganese engaged in mixed M–Mg–Mn mixed oxides (M = alkali metal) [19], two reduction peaks around 400°C and 540–600°C are attributed to the $Mn^{4+} \rightarrow Mn^{3+}$ and $Mn^{3+} \rightarrow Mn^{2+}$ reductions, respectively. The reduction maximum observed for the Mn-hexaaluminates around 540–620°C agree well with the reduction of Mn^{3+} ions incorporated in a mixed oxide matrix. For the BaMn2 and BaMn3 catalysts, however, the reduction profiles indicate that the reduction still proceeds during the temperature dwell at 1000°C, suggesting that some Mn^{3+} ions are very difficult to reduce, probably because they are located into deep positions of the spinel blocks where they are hardly accessible. These cannot be involved in the activity for methane combustion. The reduction extent of manganese at $T < 800°C$ during TPR correlates well with the catalytic activity of the solids: Fig. 6 shows the linear relationship between the rates of combustion at 550°C for the three $BaMn_x$ catalysts ($x = 1$–3) and the percentages of Mn^{3+} reduced under 800°C during TPR.

The surface composition of the substituted hexaaluminates was studied by XPS. The surface of

Table 4
Comparison of surface compositions determined by XPS with bulk compositions

Catalyst	M/Ba atomic ratio (M = Cu or Mn)	Al/Ba atomic ratio	Surface composition	Bulk composition (chemical analysis)
BaCu	1.020	8.630	$BaCu_{1.02}Al_{8.63}$	$BaCuAl_{13.3}$
BaCu2	1.741	7.657	$BaCu_{1.74}Al_{7.66}$	$BaCu_{2.1}Al_{11.9}$
BaMn	0.935	10.613	$BaMn_{0.93}Al_{10.61}$	$BaMn_{0.97}Al_{11}$
BaMn2	1.867	9.633	$BaMn_{1.87}Al_{9.63}$	$BaMn_{1.9}Al_{10}$
BaMn3	1.838	7.324	$BaMn_{1.84}Al_{7.32}$	$BaMn_{2.7}Al_{10}$
BaMn4	1.868	7.132	$BaMn_{1.87}Al_{7.13}$	$BaMn_4Al_8$

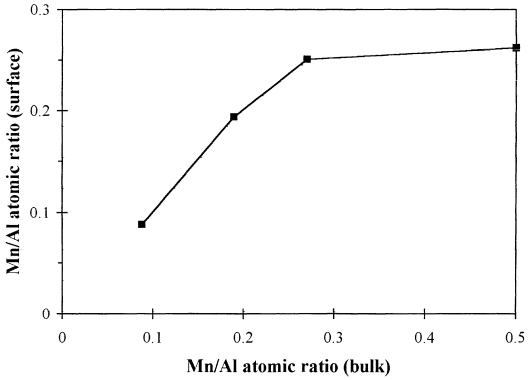

Fig. 7. Surface Mn/Al atomic ratios, determined by XPS, vs. bulk Mn/Al atomic ratios, determined by chemical analysis.

copper-based catalysts presents a deficit in Al for BaCu, and a deficit in Al + Cu for BaCu2 (Table 4). This has to be related to the presence, in the XRD patterns of these catalysts, of the α-Al_2O_3 and $CuAl_2O_4$ phases, respectively. After calcination at 1200°C, these phases should be present as large particles of low surface areas, the most important part of the surface being developed by the hexaaluminate particles which resist much better to sintering. They are thus only partially analyzed by XPS which is a surface analysis (<5 nm depth).

The surface composition of the Mn-based hexaaluminates (Table 4) was also studied by XPS. In Fig. 7, the Mn/Al surface atomic ratios are compared to the bulk Mn/Al ratios deduced from chemical analysis. The surface Mn amount increases regularly up to 3 Mn ions incorporated, but changes only very slightly when the fourth Mn cation is introduced. This is consistent with the fact that Mn_2O_3 is formed together with the hexaaluminate phase in the case of the BaMn4 catalyst, which should partially escape the XPS analysis due to the large size of the particles. In order to gain information on the oxidation state of manganese, the Mn Auger parameter was determined for the $BaMn_x$ catalysts, and compared to the values obtained for reference manganese oxides, MnO, Mn_2O_3, and MnO_2. The results are presented in Fig. 8. This figure shows that the average oxidation state of manganese tends to increase from ≈+2 to ≈+3 when the amount of manganese introduced increases. Increasing the manganese content does not only increases the number of Mn available, but also the Mn^{3+}/Mn^{2+} ratio, and thus the amount of active manganese.

3.3. Effect of ageing

The ageing treatment at 1200°C in the presence of steam leads to a decrease in the surface areas (Table 5). This confirms the strong effect of water vapor as a sintering agent, which should not be neglected in the

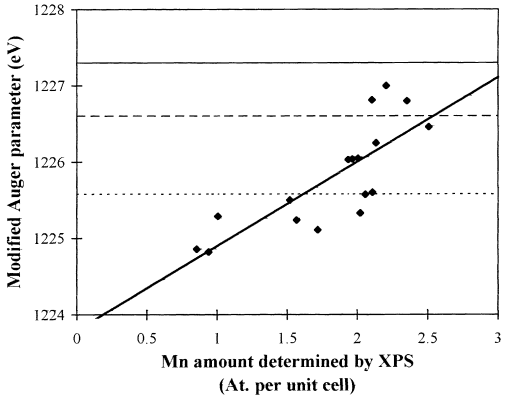

Fig. 8. Modified Auger parameters of the $BaMn_x$ catalysts (x = 1–3), vs. surface Mn amounts determined by XPS. The horizontal lines represent the values of the Auger parameters for reference Mn oxides, MnO (···), Mn_2O_3 (- - -) and MnO_2 (—).

Table 5
Specific surface areas of aged catalysts and intrinsic rates of combustion over aged and fresh catalysts

Catalyst	Surface area ($m^2\,g^{-1}$)	Rate of CH_4 combustion (mmol CH_4 $min^{-1}\,m^{-2}$)		
		500°C aged (*fresh*)	550°C aged (*fresh*)	600°C aged (*fresh*)
BaCu	6	0.483 (*0.983*)	1.142 (*2.117*)	2.283 (*3.833*)
BaMn	14	0.175 (*0.667*)	0.408 (*1.083*)	0.935 (*1.883*)
BaMn2	11	0.735 (*1.217*)	1.470 (*2.067*)	2.683 (*3.233*)
BaMn3	9	1.377 (*1.667*)	2.750 (*2.70*)	4.583 (*3.90*)
BaMn4	6	1.375 (*1.833*)	3.002 (*3.50*)	5.383 (*5.333*)

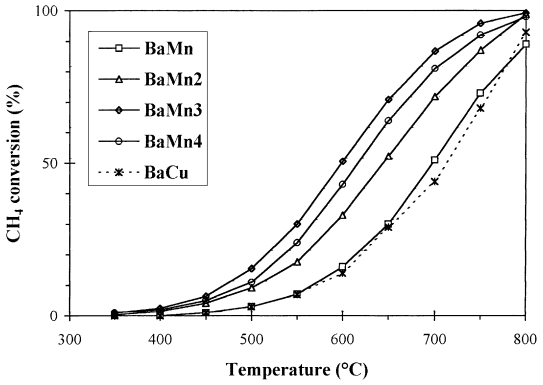

Fig. 9. Methane conversion versus temperature over the Cu- and Mn-substituted barium hexaaluminates (aged catalysts). Conditions: 1% CH_4, 4% O_2, balance N_2, total flow rate 6.4 l h^{-1}, 0.50 g catalysts.

study of thermostable materials. The phases identified in the XRD patterns, however, are not different from those of fresh catalysts.

The methane conversion temperatures are shifted to higher values, i.e. the temperatures for 50% methane conversion are now in the 600–700°C range (Fig. 9). The intrinsic rates of reaction (Table 5) are not significantly modified compared to the rates obtained with fresh catalysts, which means that there are only less surface sites available due to the lower surface areas, but these sites were not modified upon ageing. An important point to note is that the aged BaMn3 catalyst is as active as fresh BaMn. The BaMn3 composition is clearly an optimum in term of activity and resistance to thermal sintering in the presence of steam.

4. Conclusion

Copper- and manganese-substituted barium hexaaluminates were prepared by a sol–gel method, starting from metal alkoxides. Manganese and copper occupy different crystallographic sites in the hexaaluminate structure: Mn^{3+} cations are located in octahedral sites, while Cu^{2+} enters only tetrahedral positions. The Cu sites are intrinsically more active than Mn sites for methane combustion, but the copper-based catalysts are penalized by lower surface areas and by the lower limit of copper incorporation in the hexaaluminate matrix: manganese substitution for aluminium is possible up to ≈3 Mn per unit cell, while copper substitution is limited to about 1.3 Cu per unit cell. The catalytic activity of the Mn-hexaaluminates increases with Mn substitution, the BaMn3 catalyst having the optimum composition in terms of activity and resistance to ageing at 1200°C in the presence of steam. The activity of the Mn-based catalysts is directly related to the amount of reducible Mn^{3+} species incorporated in the hexaaluminate structure.

Acknowledgements

Financial support of the EEC under grant Brite-Euram 5846 is gratefully acknowledged. One of the authors (F.G.) is indebted to Pr. M. Romand, LSIS, Université Claude Bernard, Lyon, France, for access to the XPS spectrometer.

References

[1] M. Machida, K. Eguchi, H. Arai, Bull. Chem. Soc. Jpn. 61 (1988) 3659.
[2] M. Machida, K. Eguchi, H. Arai, J. Catal. 120 (1989) 377.
[3] M. Pijolat, M. Dauzat, M. Soustelle, Solid State Ionics 50 (1992) 31.
[4] B.R. Strohmeier, D.A. Hercules, J. Phys. Chem. 88 (1984) 4922.
[5] F. Gaillard, P. Artizzu, Y. Brullé, M. Primet., Surface Interface Anal. 26 (1998) 367.

[6] C.D. Wagner, L.H. Gale, R.H. Raymond, Anal. Chem. 51 (1979) 466.
[7] N. Guilhaume, M. Primet, J. Chem. Soc. Faraday Trans. 90 (1994) 1541.
[8] G. Groppi, M. Belloto, C. Cristiani, P. Forzatti, J. Solid State Chem. 114 (1995) 326.
[9] R.D. Shannon, Acta Cryst. A32 (1976) 751.
[10] D.C. Bradley, R.C. Mehrotra, D.P. Gaur, Metal Alkoxides, Academic Press, New York,1978, p. 306.
[11] J. Livage, M. Henry, C. Sanchez, Prog. Solid State Chem. 18 (1988) 259.
[12] A.G. Ersson, E.M. Johansson, S.G. Järås, Stud. Surf. Sci. Catal. 118 (1998) 601.
[13] R.M. Friedman, J.J. freeman, F.W. Lytle, J. Catal. 55 (1978) 10.
[14] G. Groppi, C. Cristiani, P. Forzatti, Preparation, characterization of hexaaluminate materials for high-temperature catalytic combustion, Catalysis 13 (1997) 85–113.
[15] H. Inoue, M. Machida, K. Eguchi, H. Arai, J. Mater. Chem. 6 (1996) 455.
[16] M.A. Zwinkels, S.G. Järås, P.G. Menon, T.A. Griffin, Catal. Rev.-Sci. Eng. 35 (1993) 319.
[17] A. Maltha, T.L.F. Favre, H.F. Kist, A.P. Zuur, V. Ponec, J. Catal. 149 (1994) 364.
[18] W. Wang, Y. Yang, J. Zhang, Appl. Catal. A: Gen. 131 (1995) 189.
[19] R. Mariscal, M.A. Peña, J.L.G. Fierro, Appl. Catal. A: Gen. 131 (1995) 243.